Article

Photochemical Bionanoreactor for Efficient Visible-Light-Driven in-vitro Drug Metabolism

Xiaoni Fang, Yaokai Duan, Yujie Liu, Gary Adkins, Weijun Zang, Wenwan Zhong, Liang Qiao, and Baohong Liu

Anal. Chem., **Just Accepted Manuscript** • Publication Date (Web): 13 Jun 2017

Photochemical Bionanoreactor for Efficient Visible-Light-Driven *in-vitro* Drug Metabolism

Xiaoni Fang,[1] Yaokai Duan,[3] Yujie Liu,[1] Gary Adkins,[3] Weijun Zang,[1] Wenwan Zhong,[3] Liang Qiao,[1, 2*] Baohong Liu[1, 2*]

1. Department of Chemistry, Institute of Biomedical Sciences and State Key Lab of Molecular Engineering of Polymers, Fudan University, Shanghai 200433, China
2. Shanghai Stomatological Hospital, Fudan University, Shanghai 200433, China
3. Department of Chemistry, University of California, Riverside 92501, United States

ABSTRACT: In light of the significance of cytochrome P450 (CYP) catalyzed drug metabolism for drug development and toxicity screening, it is very important to *in-vitro* imitate natural metabolic pathways accurately and efficiently. Herein, a novel and simple photochemical bionanoreactor has been constructed for efficient visible-light-driven *in-vitro* drug metabolism based on eosin Y functionalized macroporous ordered silica foams (MOSF-EY). Due to the unique transfer of photo-induced electrons from photosensitizers to CYP heme domain, CYP catalyzed drug metabolism can be *in-vitro* driven by the MOSF-EY nanoreactor under the irradiation of visible light. In such a case, the utilization of expensive electron donors, such as NADPH, can be avoided. Meanwhile, the *in-vitro* drug metabolism approach exhibits high efficiency due to the fast adsorption of both CYP and drug molecules from the bulk solution into the nanopores of MOSF-EY, where the enzyme and substrate are highly concentrated and confined in nanospace to achieve a high reaction rate. Taking advantage of these attractive merits, the first example of photochemical bionanoreactor has been successfully applied in *in-vitro* metabolism of both purified drug molecules and real tablets. Not only excellent CYP catalyzed drug metabolism, but also enzyme inhibition assay has been performed with the MOSF-EY photochemical bionanoreactor.

As one of the major superfamily of multifunctional monooxygenases, cytochrome P450 (CYP) is involved in a variety of metabolic reactions of endogenous and exogenous compounds in living organisms.[1-5] Since CYP involves in multi component electron transfer chains, efficient and continuous supplementation of electrons to CYP is required to maintain the catalytic cycle of CYP during drug metabolism. The cycle features the delivery of electrons from NADPH to cytochrome P450 reductase (CPR) and subsequently to CYP heme. Practical application of CYP in *in-vitro* drug metabolism is still a challenge because of the inherent low stability and activity of the enzyme, as well as the dependence on expensive NADPH and redox partners.[6-9] However, *in-vitro* CYP reactions are of great importance for drug development and toxicity screening.[10, 11] To date, the average costs of developing a new drug is ~2.5 billion US dollar, and > 90% of clinical trials of drug candidates are failed.[12-14] Therefore, the construction of a novel platform to *in-vitro* imitate the natural metabolic pathways accurately and efficiently at low cost is urgently demanded.

Great efforts have been made to imitate *in-vitro* CYP catalyzed drug metabolism, e.g. by replacing expensive NADPH with NADPH recycling systems,[15, 16] using electrochemistry methods,[17-19] or employing light-activated approaches.[6] The use of NADPH recycling systems is of scientific interests, but suffers from the low tolerance of monooxygenases toward peroxides, which results in rapid inactivation of the monooxygenases. Electrochemically-driven CYP catalyzed drug metabolism relies on the direct electron transfer between CYP and electrode, which has turned out to be a cost-effective method. However, it is difficult to achieve the direct electron transfer to the deeply buried iron-heme centers of CYP. In addition, the stability and activity of CYP are limited on bare electrodes. Therefore, cumbersome procedures, such as the modification of electrodes, are inevitable. Among all the alternative strategies, light driven CYP-mediated drug metabolism has drawn significant attention during the last few years. For instance, quantum dots, eosin Y and Ru(II) photosensitizer have been used as electron suppliers for drug metabolism.[6, 20-22] However, the reported light-driven drug metabolism methods exhibit slow kinetics in bulk solution reaction, leading to inefficient metabolism and identification of metabolites at low concentrations of CYP or drugs. The aforementioned shortcomings should be overcome in terms of the urgent need of highly efficient *in-vitro* CYP catalyzed drug metabolism approaches.

Nanoreactors have attracted great attentions and offered distinctive advantages in enzymatic catalysis.[23-27] For example, Liu et al. have developed electrochemistry driven TiO_2 nanotube arrays for the study of enzyme biocatalysis and drug metabolism.[31] Recently, mesoporous materials, such as macroporous ordered silica foams (MOSF), have been reported as excellent candidates of enzymatic nanoreactors.[28-30] Benefiting from their relatively large pore sizes and excellent biocompability, mesoporous materials have been employed to pre-immobilize high concentration of enzymes and substrates within the nanopores and confine enzymatic reactions in nanoscale domains.[23,28] With theoretical predictions and experimental validations, we have previously demonstrated that mesoporous materials can offer distinctive advantages in hosting CYP catalyzed drug metabolism, including fast reaction kinetics, minimal consumption of multiple enzymes, good stability, and rapid separation of products from metabolic reaction systems.[24] However, mesoporous materials have not been extensively exploited for light-driven CYP catalyzed drug metabolism. It's then desirable to design a photochemical nanoreactor, which can realize

NADPH- and reductase-free, light-driven, and highly efficient CYP catalyzed *in-vitro* drug metabolism.

Herein, a novel and simple photochemical bionanoreactor has been constructed by introducing eosin Y (EY) modified macroporous ordered silica foams (MOSF-EY) as hosts for visible-light-driven and CYP catalyzed drug metabolism. By introducing the remarkable photosensitizer EY in the macroporous frameworks of MOSF, MOSF-EY not only serves as an electron supplier, but also a bionanoreactor for drug metabolism. The bionanoreactor, in fact, offers abundant electrons for metabolic reaction and facilitates their access to CYP's heme domain. Therefore, the efficiency of *in-vitro* drug metabolism can be significantly enhanced. As a proof-of-concept of the approach, purified drug molecules and real tablets were chosen as substrates. Both faster reaction kinetics and higher conversion ratio were achieved compared to traditional *in-vitro* drug metabolism system by NADPH. Furthermore, enzyme inhibition assay has also been realized with the MOSF-EY photochemical bionanoreactor. All the results demonstrate that such a photochemical bioreactor can offer a clinically relevant approach with potential application in efficient drug candidates screening and thereby the development of new drugs.

EXPERIMENTAL SECTION

Chemicals. Cytochrome P450 CYP3A4 expressed in E. coli (human, recombinant), cytochrome P450 CYP3A4 isozyme microsomes expressed in baculovirus-infected insect cells (human, recombinant) with cytochrome P450 reductase and cytochromeb5, cytochrome P450 reductase (human, recombinant) expressed in baculovirus infected insect cells, reduced nicotinamide adenine dinucleotide phosphate (NADPH), nifedipine (⩾98%, powder), caffeine (⩾99%, powder), tetramethyl orthosilicate (TMOS, ⩾ 99%), EO20PO70EO20 (P123, where EO is poly(ethylene oxide) and PO is poly(propylene oxide), dry toluene, (3-aminopropyl) triethoxysilane (APTES), eosin Y (⩾90%) were purchased from Sigma Chemical Co. (St. Louis, MO, USA). Methanol, acetonitrile, and methylene chloride were purchased from Dikma Technologies Inc. (Lake Forest, CA). Testosterone (⩾98%), ketoconazole (⩾98%), sodium sulphate anhydrous, sodium acetate anhydrous, acetic acid were obtained from Sinopharm Chemical Reagent Co. (Shanghai, China). The stock solutions of drugs and caffeine were prepared in methanol. NADPH was prepared in potassium phosphate (PB) buffer, 0.1 M, pH = 8.0. All reagents were used as received without further purification. Deionized water (18.2 MΩ cm) used for all experiments was obtained from a Milli-Q system (Millipore, Bedford, MA).

Synthesis and Characterization of MOSF-EY Materials. MOSF materials were synthesized according to a previously reported method.[32] Briefly, 1.00 g of P123 and 1.7 g of Na2SO4 were dissolved in 30 mL of NaAc-HAc buffer solution (0.02 M, pH=5.0) to form a homogenous solution under stirring at 35 °C. And then 1.52 g of TMOS was added to the solution under stirring. After 5 minutes, the stirring was stopped. The resultant mixture was hydrothermally treated at 100 °C for another 24 h after keeping static for 24 h. The resulting white precipitates were filtered, washed thoroughly by water to remove any salts, and then dried at room temperature. The final MOSF products were obtained after baking the white precipitates at 550 °C for 5 h.

MOSF was functionalized with amino groups. In a standard modification process, APTES was used as coupling agent.[33] MOSF materials were firstly dried and degassed at 110 °C, and then dispersed in dry toluene (0.1 g MOSF in 30 g toluene). An excess of APTES (3 mL) was added under stirring and the mixture was stirred and refluxed for 24 h at 110 °C. The resulting solid was filtered and washed sequentially by toluene, dichloromethane and ethanol three times, respectively. The final NH2-MOSF products were obtained after through drying at 70 °C overnight. Finally, 10 μg EY and 20 μg NH_2-MOSF were added in PB buffer with a final volume of 100 μL and stirred for 10 min at room temperature, followed by centrifugation and washing by deionized water thoroughly to obtain the MOSF-EY materials.

Scanning electron microscope (SEM) images were obtained by SUPERSCAN SSX-550 scanning electron microscope (Shimadzu, Japan). Transmission electron microscopy (TEM) images were obtained with a JEOL 2011 microscope operated at 200 kV (JEOL, Tokyo, Japan). Samples for TEM measurements were suspended in ethanol and supported on a carbon-coated copper grid. The infrared spectra were obtained using an FT-IR360 (Nicolet, Thermo Scientific). Cyclic voltammetric experiments were performed with a CHI 660C electrochemical analyzer (CH Instruments) with a conventional three-electrode configuration, where modified glassy carbon electrode (GCE) with the diameter of 3 mm was employed as working electrode, Pt wire served as counter electrode, and a saturated calomel electrode (SCE) was used as reference electrode. A green lamp was used as the irradiation source to initiate CYP catalyzed drug metabolism (λ: 534 ± 5 nm, P: <80 mW, Φ: 22X90 mm).

Visible-Light-Driven CYP Catalyzed Drug Metabolism by the MOSF-EY Photochemical Bioreactor. The visible-light-driven metabolism by the MOSF-EY bionanoreactor was conducted in a microcentrifuge tube (1.5 mL) at 37 °C. Quantitative reaction mixture consisted of CYP (5 μL), MOSF-EY (20 μg), and nifedipine (4 μg) or testosterone (2 μg) in 20 μL of potassium phosphate (PB, 0.1 M)-TEOA (0.1 M) buffer (pH ≈8.0). It is noteworthy that TEOA serves as an electron donor in the light driven CYP catalyzed drug metabolism. For metabolic reaction, the mixture was pre-incubated at 37 °C for 5 min for the adsorption of substrates. Green lamp was employed to initiate the oxidation reaction. After being incubated at 37 °C for a certain period, the reaction was quenched by the addition of ice–methylene chloride. At the same time, the drug molecules with their metabolites were extracted by methylene chloride, the detailed process was introduced in Supporting Information. At last, methylene chloride was dried under a N_2 stream without heating, and the dried samples were redissolved in methanol for further

analysis. We also carried out the same reaction for 10 min without EY, TEOA, or green light as control experiments.

When the metabolism of nifedipine sustained-release tablets was studied, a similar method was used. 5 μL CYP, 20 μg MOSF-EY materials, and 10 μg nifedipine sustained-release tablets were added in 20 μL of potassium phosphate (PB, 0.1 M)-TEOA (0.1 M) buffer (pH ≈8.0) and then incubated at 37 °C for a certain period. Before HPLC–MS analysis, the extracted samples were centrifuged to remove precipitates thoroughly.

In-vitro metabolism of nifedipine assisted by NADPH way was also performed.[34] Briefly, 4 μg of nifedipine was dissolved in PB buffer (0.1 M). After the addition of CYP (5 μL) and cytochrome P450 reductase (5 μL) of microsomes (10 μL), the mixture was pre-incubated at 37 °C for 5 min. Then 60 μg of NADPH was added to the solution to initiate the oxidation reaction for 10 minutes. Finally, the metabolites were extracted, redispersed, and analyzed by HPLC–MS.

Chemical Inhibition Study. Chemical inhibition studies were performed by adding ketoconazole to the incubation mixture of nifedipine or testosterone before the irradiation of green light.

LC–MS Analysis. For rapid screening of reactive metabolites, the reaction mixture was analyzed by HPLC–MS. Samples were first subjected to chromatographic separation with an Agilent series 1260 HPLC system (Agilent Technologies, Palo Alto, CA) integrated with an autosampler and a UV detector. 20 μL of sample solution was injected into a VP-ODS C18 column (250 mm × 4.6 mm i.d., 5μm, Agilent) at the flow rate of 0.6 mL/min. The detailed separation process is explained in the Supporting Information. The fractions from LC were introduced into a 6460 QQQ mass spectrometer (Agilent) that was operated in positive ion mode under optimized parameter conditions (refer to the Supporting Information). The structure information on reactive metabolites can be deduced from tandem MS spectra. Additionally, for quantitative analysis of the metabolites, 20 μL of caffeine (0.1 μg/μL) was added as an internal standard before HPLC-MS analysis.

RESULTS AND DISCUSSION

Construction and optimization of the EY-MOSF photochemical bionanoreactor. The EY-MOSF bionanoreactor was constructed and optimized for efficient visible-light-driven CYP catalyzed *in-vitro* drug metabolism. The chemical modification of MOSF with EY (MOSF/EY ratio of 10:1 (w/w)) was validated by Fourier transform infrared (FT-IR) spectroscopy. In Figure 1a, the absorption peak of MOSF at 1083 cm^{-1} is ascribed to the stretching vibration of –Si–O. In the case of amino modified MOSF (Figure 1b), the peaks around 1568 and 2931 cm^{-1} can be attributed to the grafted -NH2 groups and -CH_2- groups of silica coupling agent (APTS), respectively. After modification with EY (Figure 1c), new bands at 1456 cm^{-1} and 1557 cm^{-1} correspond to aromatic C=C stretching of EY. In addition, FT-IR bands at 1351 and 1616 cm^{-1} are assigned to aliphatic C–O stretching and N-H bending of EY. These results gave strong evidence about the successful covalent binding of EY to the amino modified MOSF.

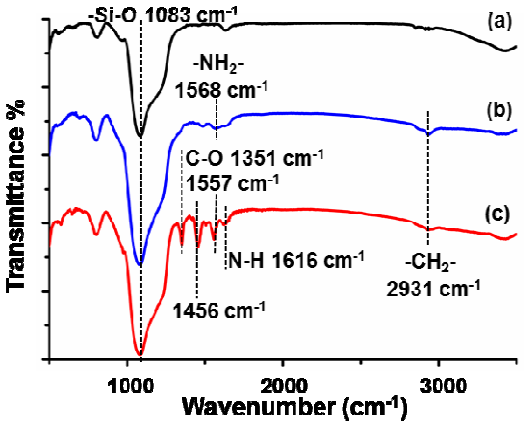

Figure 1. FTIR spectra of (a) MOSF, (b) NH_2-MOSF and (c) MOSF-EY.

The morphology and structure of MOSF-EY were further validated by SEM and TEM. Figure 2a&b display the SEM images of MOSF-EY. Compared to MOSF (Figure S1), the foam-like structure can be well-preserved after surface modification with EY, and the pore size is still ~100 nm. The TEM images also reveal the foam structure of MOSF-EY with hexagonal column assemblies (Figure 2c). From both SEM and TEM, no large aggregates were observed for MOSF-EY, suggesting the well-dispersed state of EY species. As shown in Table S1, MOSF has a surface area of 351 m^2/g and pore volume of 1.25 cm^3/g, whereas the surface area and pore volume of MOSF-EY decrease to 298 m^2/g and 1.09 cm^3/g, respectively, which can be attributed to the impregnation of EY on the surface of MOSF. The ζ potentials of MOSF and NH_2-MOSF were measured as –35.6 and +17.5 mV in 0.1 M PB buffer (pH ≈ 8.0), respectively, indicating the successful modification of MOSF by APTES. Thus, NH_2-MOSF was positively charged that can be served as an adsorbent for anionic EY through the charge interaction between NH_2-MOSF and EY. After the modification of EY on NH_2-MOSF, the ζ potential of MOSF-EY decreased to –5.1 mV due to the modification of the negatively charged EY on the surface of NH_2-MOSF, further demonstrating the structure of MOSF-EY.

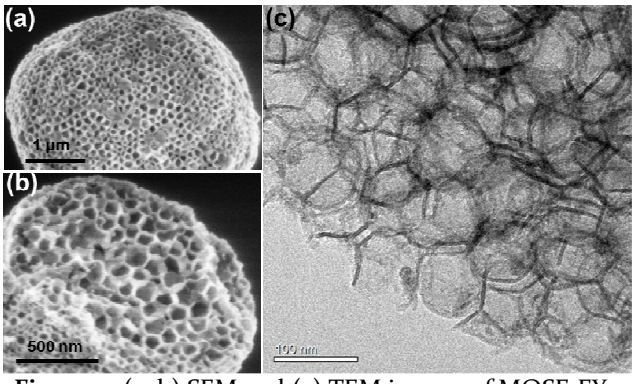

Figure 2. (a, b) SEM and (c) TEM images of MOSF-EY.

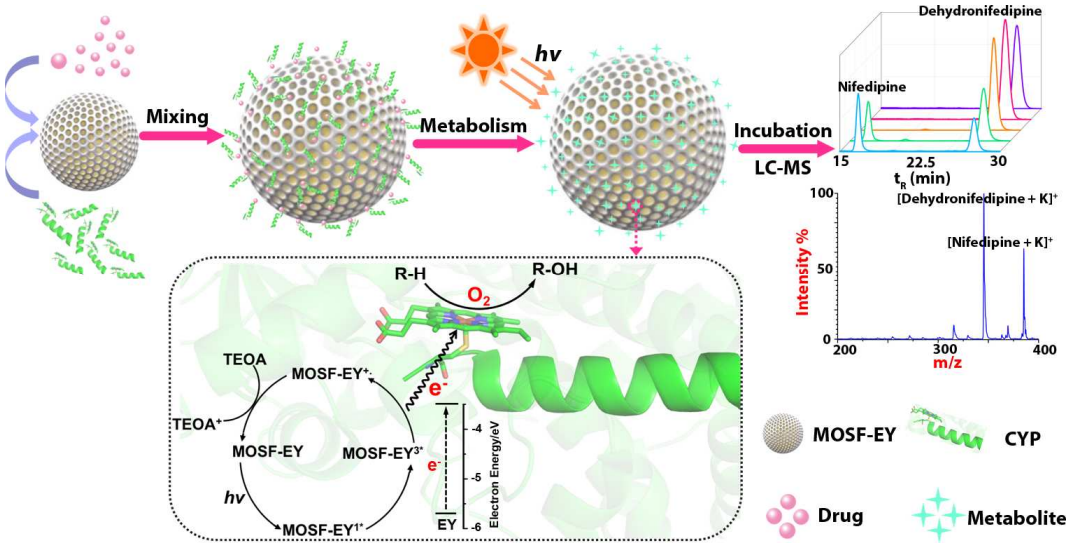

Scheme 1. Schematic illustration of the MOSF-EY photochemical bionanoreactor assisted light-driven efficient drug metabolism.

Considering that the absorbance of MOSF-EY materials to visible light is relevant to the amount of EY, a series of MOSF-EY materials were fabricated by varying the amount of EY in order to construct a photochemical bioreactor with excellent performance in CYP catalyzed drug metabolism. The amount of EY ranging from 0 to 200 μg was used to modify MOSF (1 mg). As shown in Figure S2, the maximum absorbance of MOSF-EY to light with the wavelength from 520 to 600 nm was observed when the EY amount was 100 μg/ mg MOSF. Further increase of the amount of EY could not lead to a better light harvesting. Therefore, the MOSF-EY material with a final MOSF/EY ratio of 10:1 (w/w) was applied to assist visible-light-driven CYP catalyzed *in-vitro* drug metabolism.

EY-MOSF as a photochemical bionanoreactor for CYP catalyzed drug metabolism. As illustrated in Scheme 1, MOSF-EY serves not only as an electron supplier but also a bionanoreactor for highly efficient CYP catalyzed drug metabolism. The process is a series of reactions confined in nanospaces, including: (i) enrichment of drug and CYP in the nanopores of MOSF-EY; (ii) excitation of electrons from the highest occupied molecular orbital (HOMO) to the lowest unoccupied molecular orbital (LUMO) of MOSF-EY under the irradiation of visible light. MOSF-EY will obtain photons and produce single excited state MOSF-EY1*, and subsequently triplet excited state MOSF-EY3* are produced during the process; (iii) transfer of the photoexcited electrons from MOSF-EY LUMO to CYP heme to induce CYP catalyzed drug metabolism; (iv) reduction of the oxidized MOSF-EY to its ground state by triethanolamine (TEOA).

The interaction between MOSF-EY and CYP is essential for the electron transfer reactions during the light-driven drug metabolism. Spectrophotometry and cyclic voltammetry were performed to investigate the electron transfer process between MOSF-EY and CYP heme. Significant red-shift in spectrophotometry could be observed when EY is bound to proteins.[35] As expected, the color change from red to yellow of MOSF-EY was observed after the addition of CYP, corresponding to the red-shift of the absorption peak of MOSF-EY at 537 nm, Figure 3a. Benefiting from the interaction between MOSF-EY and CYP and the outstanding absorbance of MOSF-EY to visible light, the reduction potential of CYP shifted significantly from −0.68 V to −0.77 V (Figure 3b) under light irradiation. The negative shift is a result of the co-

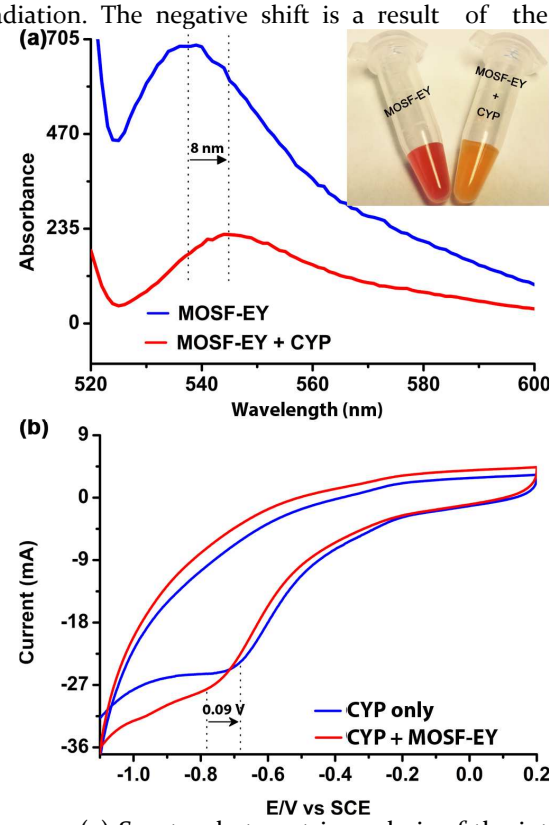

Figure 3. (a) Spectrophotometric analysis of the interaction between MOSF-EY and CYP. (b) Cyclic voltammetric measurement of CYP modified electrode in the absence and presence of MOSF-EY. SCE: saturated calomel electrode.

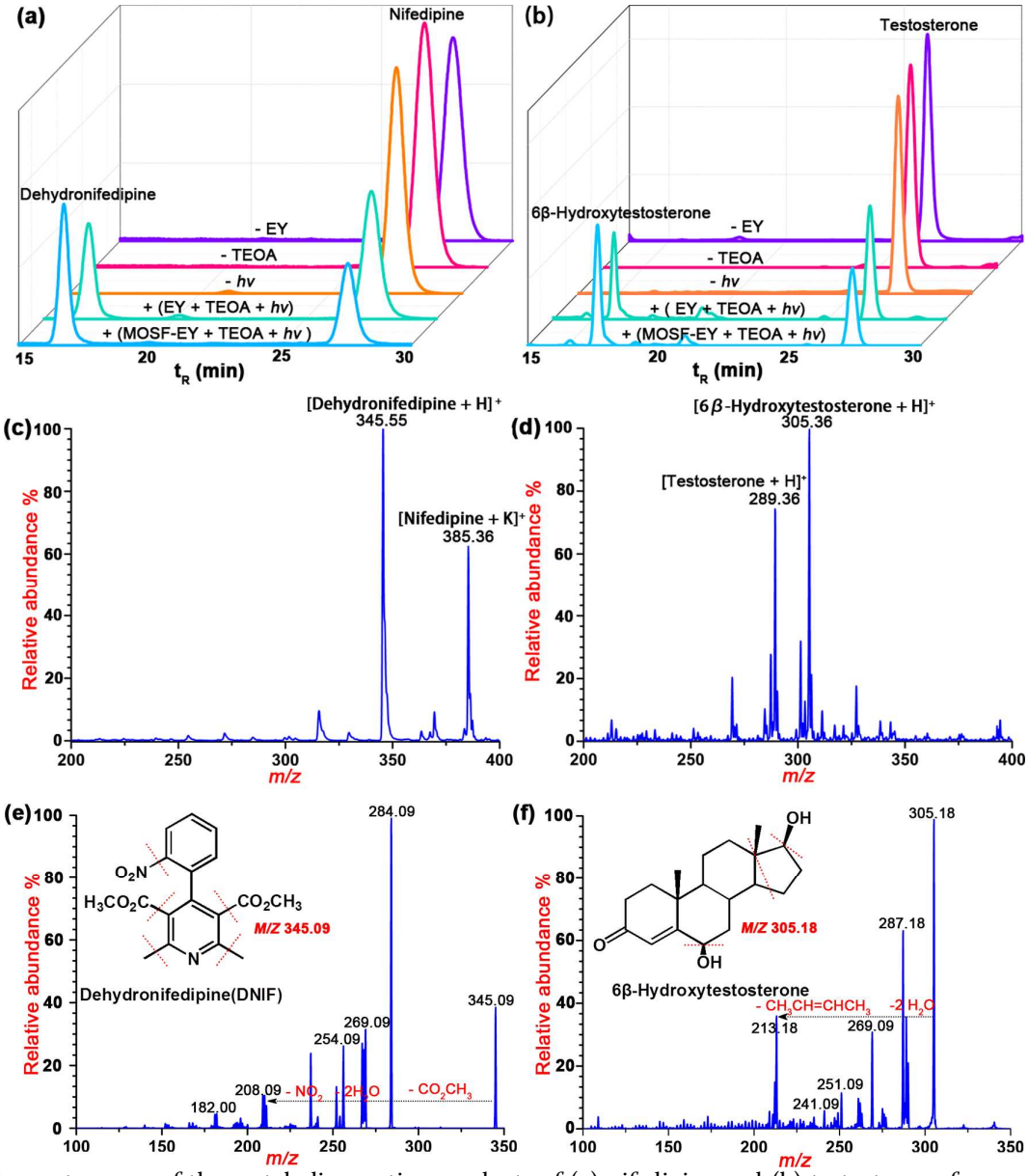

Figure 4. Chromatograms of the metabolic reaction products of (a) nifedipine and (b) testosterone from 10 min of CYP catalyzed metabolism under various experimental conditions as indicated on the figures. Mass spectra of (c) nifedipine and (d) testosterone metabolism with the assistance of MOSF-EY photochemical bionanoreactor. Tandem MS by CID of (e) the peak at m/z=345 on Figure 4(c), and (f) the peak at m/z=305 on Figure 4(d).

reduction of EY and CYP, confirming the presence of electron transfer from MOSF-EY to CYP. During the EC measurement, CYP was immobilized on the electrode. Therefore, only EY on the surface of MOSF may react with the immobilized CYP. Nevertheless, the reaction between CYP and EY under light irradiation was demonstrated. Thus, MOSF-EY can be used as an excellent photochemical bionanoreactor towards CYP catalyzed drug metabolism.

Metabolism of nifedipine and testosterone assisted by the EY-MOSF photochemical bionanoreactor. To demonstrate the feasibility of the proposed protocol, the MOSF-EY photochemical bionanoreactor was used to assist the metabolism of nifedipine and testosterone catalyzed by CYP. For direct comparison, metabolic reaction in bulk solution was carried out with the same amount of CYP and substrates. The chromatography in Figure 4 shows the results of nifedipine and testosterone metabolism with and without the assistance of MOSF-EY under different conditions. As illustrated on Figure 4a, the peaks with retention time (RT) at 17 and 27 min can be attributed to dehydronifedipine and nifedipine, respectively. For testosterone, the major metabolite was observed at 18 min. No metabolite of nifedipine or testosterone can be detected in the absence of EY, TEOA or visible-light, indicating that the electron pairs and light source are indispensable for light-driven CYP catalyzed drug metabolism. Moreover, CYP catalyzed drug metabolism can be performed more efficiently with the MOSF-EY photochemical bionanoreactor. The amounts of generated metabolites were much larger than that obtained after 10 min of in-bulk-solution metabolism by EY, TEOA and

visible-light irradiation. Figure 4c&d show the corresponding mass spectra of nifedipine, testosterone and their metabolic reaction products obtained by the MOSF-EY photochemical bioreactor. The structure of the metabolic products of nifedipine and testosterone were confirmed by tandem MS (Figure 4e&f). Both the molecular weight and fragments indicated the generation of dehydronifedipine and 6β-hydrotestosterone.

The reaction kinetics of drug metabolism assisted by MOSF-EY is mainly dependent on the amount of immobilized CYP, affinity between enzyme and substrate, the pore size of MOSF-EY, and the enzymatic activity. Kinetic data were obtained using the Michaelis-Menten model. The detailed calculations of K_M & V_{max} values were illustrated in Supporting Information. Benefiting from the large pore size and negatively charged surface, MOSF-EY photochemical bionanoreactor shows highly fast adsorption kinetics and high loading capacity to the positively charged CYP in potassium phosphate (PB) buffer, pH =8.0.

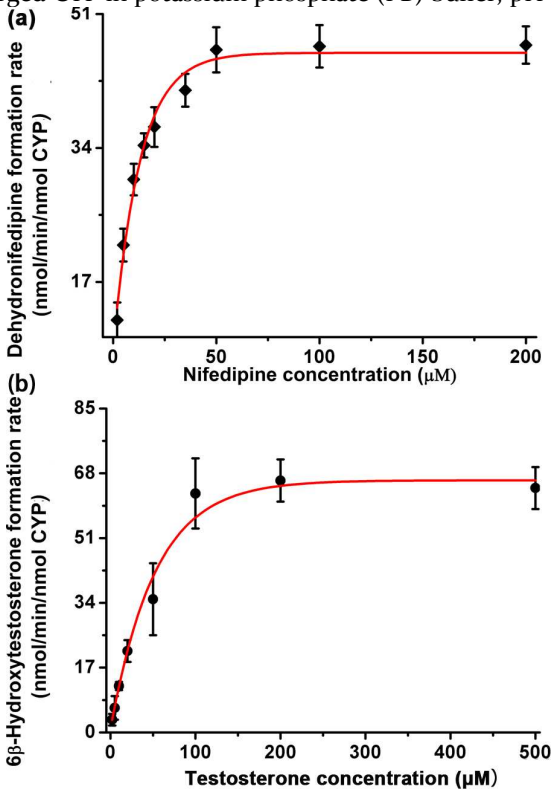

Figure 5. Michaelis-Menten plots for CYP catalyzed (a) nifedipine (0-200 μM) and (b) testosterone (0-500 μM) metabolism assisted by the MOSF-EY photochemical bionanoreactor. Metabolic reactions were performed with 5 μL CYP in 0.1 mL potassium phosphate (PB, 0.1 M)-TEOA (0.1 M) buffer for 10 min. Error bar shows the standard deviation (n=3).

As demonstrated in Figure S4 (Supporting Information), about 88% of the maximum adsorption amount of CYP could be achieved within 2 min. The introduction of the bionanoreactor in CYP catalyzed drug metabolism not only dramatically in-creases the local concentration of CYP, but also facilitates the access of substrates to CYP. As shown in Figure 5 and Table S2 (Supporting Information), the K_m for nifedipine and testosterone metabolism are 5.06 ± 0.45 μM and 53.37 ± 4.01 μM, respectively, which are much lower than previously reported methods, indicating that the immobilized CYP has good affinity to substrates.[36-40] Moreover, the apparent V_{max} values for nifedipine and testosterone metabolism assisted by the MOSF-EY photochemical bionanoreactor are 47.09 ± 1.10 and 74.15 ± 5.92 nmol/min/nmol CYP, respectively, much larger than those described in previous reported approaches.[36,41] The large V_{max} values in our photochemical system come from the enhanced activity of enzymes in confined nanospace, demonstrating that the MOSF-EY bionanoreactor can provide a suitable microenvironment to maintain the stability and catalytic activity of enzymes. All of these results indicate that CYP catalyzed drug metabolism assisted by MOSF-EY is highly advantageous in enhancing metabolic reaction kinetics.

To further confirm the efficiency of the MOSF-EY photochemical bionanoreactor in CYP catalyzed drug metabolism, the absolute amount of metabolites of nifedipine and testosterone were determined and compared to other *in-vitro* drug metabolism methods. As shown in Table 1, a total of 48.60 ± 3.97 nmol dehydronifedipine and 26.09 ± 4.31 nmol 6β-dehydroxytestosterone were obtained based on the MOSF-EY photochemical bioreactor, which are much more than traditional in-bulk-solution metabolism of the same amount of substrates relying on the consumption of expensive NADPH and reductase. Even when microsomes containing CYP and CPR were used to drive the metabolism of nifedipine and testosterone in solution, the amount of generated metabolites was still much less than the MOSF-EY approach. Such a difference in drug metabolism is likely due to the improved efficiency of electron transfer in the MOSF-EY system compared to bulk solution reactions, and the nanoconfinement effect of enzymatic reaction in nanospaces. The improvement of absolute amount of metabolites plays a key role in drug screening, especially for complex and trace drugs. Such advances will contribute to the development of drug with desired safety and efficiency.

Encouraged by the prominent features of the proposed protocol, the MOSF-EY photochemical bionanoreactor was further applied to the *in-vitro* metabolism of nifedipine sustained release tablets. The UV–HPLC chromate-

Table 1. Summary of the Absolute Amount of Metabolites Obtained by Different Strategy (n=3)

metabolism strategy	Dehydronifedipine(nmol)	6β-dehydroxytestosterone (nmol)
MOSF-EY nanoreactor/CYP4A4/hv	48.60 ± 3.97	26.09 ± 4.31
EY/CYP3A4/hv	25.69 ± 5.28	21.35 ± 2.92
CYP3A4/CPR/NADPH	15.06 ± 4.26	12.18 ± 3.50
CYP3A4 microsome/NADPH	24.02 ± 2.83	18.84 ± 5.17

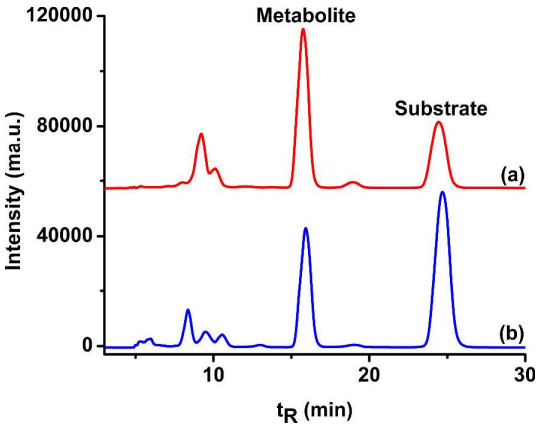

Figure 6. Chromatograms of 30 min nifedipine sustained-release tablets oxidation activated by the (a) MOSF-EY and (b) NADPH in solution system. Metabolic reactions were performed with 5 μL CYP, 10 μg nifedipine sustained-release tablets in 20 μL of potassium phosphate (PB, 0.1 M)-TEOA (0.1 M) buffer for 30 min with and without the assistance of MOSF-EY photochemical bioreactor.

grams in Figure 6 illustrate the results of nifedipine sustained release tablets oxidation activated by NADPH and the MOSF-EY photochemical system, respectively. More than 2/3 nifedipine could be consumed after 30 min with the MOSF-EY photochemical bioreactor, whereas only 1/3 nifedipine were consumed under the same condition by the NADPH based in solution reaction system. The result clearly indicates that MOSF-EY can be used as a simple and efficient photochemical bioreactor for the *in-vitro* metabolism of complex samples.

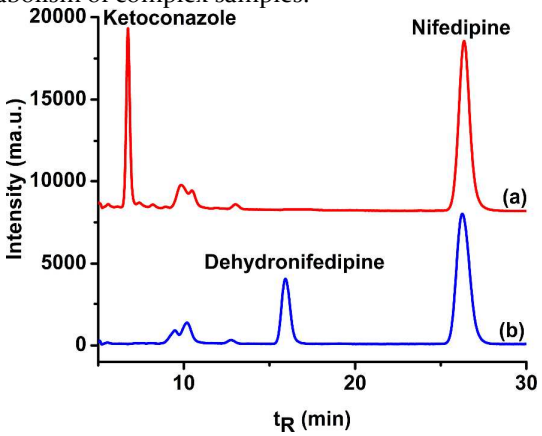

Figure 7. UV-HPLC chromatograms of nifedipine metabolism assisted by the MOSF-EY photochemical bioreactor (a) without and (b) with the presence of ketoconazole. Metabolic reactions were performed with 5 μL CYP, 4 μg nifedipine, 1 μM ketoconazole in 20 μL of potassium phosphate (PB, 0.1 M)-TEOA (0.1 M) buffer for 30 min with the assistance of MOSF-EY photochemical bionanoreactor.

The inhibition effect of drugs on CYP activity is clinically significant for the development of pharmaceutical drugs and the assessment of their toxicity. To determine whether the developed MOSF-EY photochemical bionanoreactor can be applied to enzyme inhibition analysis, MOSF-EY assisted CYP catalyzed drug metabolism was carried out in the presence of ketoconazole, a commonly used inhibitor of CYP mediated nifedipine metabolism. As shown in Figure 7, there is not any dehydronifedipine determined after the addition of ketoconazole, indicating that ketoconazole is still an active inhibitor of CYP in the MOSF-EY photochemical bionanoreactor based *in-vitro* metabolism system. All these superiorities render the MOSF-EY photochemical bionanoreactor based *in-vitro* metabolism as a novel clinically relevant biotechnological approach with potential application in efficient drug screening and the development of new drugs.

CONCLUSIONS

In summary, we have demonstrated that CYP catalyzed drug metabolism can be effectively carried out in the absence of expensive NADPH and redox partner based on the MOSF-EY photochemical bionanoreactor under visible light illumination. MOSF-EY materials inherit the virtues of photosensitizer and nanoreactor, thereby act as both an electron supplier and a bionanoreactor. With the MOSF-EY photochemical bionanoreactor, much faster *in-vitro* metabolic reaction kinetics is obtained. It is anticipated that the novel and simple MOSF-EY photochemical bionanoreactor for visible-light-driven drug metabolism would lead to promising advance in new drug development with desired safety and therapeutical efficiency.

ASSOCIATED CONTENT

Supporting Information

Detailed descriptions of the LC–MS experiments, data for the absorbance of MOSF-EY materials relevant to the amount of EY, structure of MOSF, and adsorption kinetic of CYP by MOSF-EY. This material is available free of charge via internet at http://pubs.a.org/.

AUTHOR INFORMATION

Corresponding Author

*E-mail: bhliu@fudan.edu.cn. Fax:(+86) 21-6564-1740
*E-mail: liang_qiao@fudan.edu. Fax:(+86) 21-6564-1740

Notes

The authors declare no competing financial interest.

ACKNOWLEDGMENT

This work was supported by NSFC (21175028, 21375022 and 21105014). LQ would also like to thank the Thousand Talents Program and NSFC (81671849) for support.

REFERENCES

(1) Meunier, B.; de Visser, S. P.; Shaik, S. *Chem. Rev.* **2004**, *104*, 3947-3980.
(2) Denisov, I. G.; Makris, T. M.; Sligar, S. G.; Schlichting, I. *Chem. Rev.* **2005**, *105*, 2253-2278.
(3) Krishnan, S.; Wasalathanthri, D.; Zhao, L.; Schenkman, J. B.; Rusling, J. F. *J. Am. Chem. Soc.* **2011**, *133*, 1459-1465.

(4) Wang, N.; Gao, C.; Xue, F.; Han, Y.; Li, T.; Cao, X.; Zhang, X.; Zhang, Y.; Wang, Z. L. *ACS Nano* **2015**, *9*, 3159-3168.
(5) Newcomb, M.; Zhang, R.; Chandrasena, R. E. P.; Halgrimson, J. A.; Horner, J. H.; Makris, T. M.; Sligar, S. G. *J. Am. Chem. Soc.* **2006**, *128*, 4580-4581.
(6) Tran, N.-H.; Nguyen, D.; Dwaraknath, S.; Mahadevan, S.; Chavez, G.; Nguyen, A.; Dao, T.; Mullen, S.; Nguyen, T.-A.; Cheruzel, L. E. *J. Am. Chem. Soc.* **2013**, *135*, 14484-14487.
(7) Mie, Y.; Suzuki, M.; Komatsu, Y. *J. Am. Chem. Soc.* **2009**, *131*, 6646-6647.
(8) Krishnan, S.; Schenkman, J. B.; Rusling, J. F. *J. Phys. Chem. B* **2011**, *115*, 8371-8380.
(9) Odijk, M.; Olthuis, W.; van den Berg, A.; Qiao, L.; Girault, H. *Anal. Chem.* **2012**, *84*, 9176-9183.
(10) Lee, M.-Y.; Park, C. B.; Dordick, J. S.; Clark, D. S. *Proc. Natl. Acad. Sci. U. S. A.* **2005**, *102*, 983-987.
(11) Mario Geysen, H.; Schoenen, F.; Wagner, D.; Wagner, R. *Nat. Rev. Drug Discovery* **2003**, *2*, 222-230.
(12) Paul, S. M.; Mytelka, D. S.; Dunwiddie, C. T.; Persinger, C. C.; Munos, B. H.; Lindborg, S. R.; Schacht, A. L. *Nat. Rev. Drug Discovery* **2010**, *9*, 203–214.
(13) Harper, A. R.; Topol, E. J. *Nat. Biotechnol.* **2012**, *30*, 1117–1124.
(14) Lazonick, W.; Tulum, O. Res Policy 2011, 40, 1170–1187.
(15) van der Donk, W. A.; Zhao, H. *Curr. Opin. Biotechnol.* **2003**, *14*, 421-426.
(16) Hollmann, F.; Hofstetter, K.; Schmid, A. *Trends Biotechnol.* **2006**, *24*, 163-171.
(17) Yoshioka, K.; Kato, D.; Kamata, T.; Niwa, O. *Anal. Chem.* **2013**, *85*, 9996-9999.
(18) Fantuzzi, A.; Fairhead, M.; Gilardi, G. *J. Am. Chem. Soc.* **2004**, *126*, 5040-5041.
(19) Wirtz, M.; Klucik, J.; Rivera, M. *J. Am. Chem. Soc.* **2000**, *122*, 1047-1056.
(20) Park, J.; Lee, S.; Cha, G.; Choi, D.; Nam, D.; Lee, J.; Lee, J.; Yun, C.; Jeong, K.; Park, C. *Angew. Chem., Int. Ed.* **2015**, *54*, 969–973.
(21) Xu, X.; Qian, J.; Yu, J.; Zhang, Y.; Liu, S. *Chem. Commun.* **2014**, *50*, 7607-7610.
(22) Qian, J.; Zhu, W.; Mi, L.; Xu, X.; Yu, J.; Cui, D.; Xue, Y.; Liu, S. *J. Electrochem. Commun.* **2014**, *733*, 27-32.
(23) Qian, K.; Wan, J.; Liu, F.; Girault, H. H.; Liu, B.; Yu, C. *ACS Nano* **2009**, *3*, 3656-3662.
(24) Fang, X.; Zhang, P.; Qiao, L.; Feng, X.; Zhang, X.; Girault, H. H.; Liu, B. *Anal. Chem.* **2014**, *86*, 10870-10876.
(25) Liu, Y.; Wang, Y.; Wang, Y.; Lu, J.; Piñón, V.; Weck, M. *J. Am. Chem. Soc.* **2011**, *133*, 14260-14263.
(26) Fang, X.; Liu, Z.; Hsieh, M.-F.; Chen, M.; Liu, P.; Chen, C.; Zheng, N. *ACS Nano* **2012**, *6*, 4434-4444.
(27) Fang, X.; Qiao, L.; Yan, G.; Yang, P.; Liu, B. *Anal. Chem.* **2015**, *87*, 9360-9367.
(28) Qian, K.; Wan, J.; Qiao, L.; Huang, X.; Tang, J.; Wang, Y.; Kong, J.; Yang, P.; Yu, C.; Liu, B. *Anal. Chem.* **2009**, *81*, 5749-5756.
(29) Gan, J.; Zhu, J.; Yan, G.; Liu, Y.; Yang, P.; Liu, B. *Anal. Chem.* **2012**, *84*, 5809-5815.
(30) Gasilova, N.; Srzentić, K.; Qiao, L.; Liu, B.; Beck, A.; Tsybin, Y. O.; Girault, H. H. *Anal. Chem.* **2016**, *88*, 1775-1784.
(31) Lu, J.; Li, H.; Cui, D.; Zhang, Y.; Liu, S. *Anal. Chem.* **2014**, *86*, 8003-8009.
(32) Wang, H.; Zhou, X.; Yu, M.; Wang, Y.; Han, L.; Zhang, J.; Yuan, P.; Auchterlonie, G.; Zou, J.; Yu, C. *J. Am. Chem. Soc.* **2006**, *128*, 15992-15993.
(33) Descalzo, A. B.; Jimenez, D.; Marcos, M. D.; Martínez-Máñez, R.; Soto, J.; El Haskouri, J.; Guillém, C.; Beltrán, D.; Amorós, P.; Borrachero, M. V. *Adv. Mater.* **2002**, *14*, 966-969.
(34) Sohl, C. D.; Cheng, Q.; Guengerich, F. P. *Nat. Protoc.* **2009**, *4*, 1252-1257.
(35) Waheed, A. A.; Rao, K. S.; Gupta, P. D. *Anal. Biochem.* **2000**, *287*, 73-79.
(36) Zhang, J.; Hoogmartens, J.; Van Schepdael, A. *Electrophoresis* **2008**, *29*, 3694-3700.
(37) Fantuzzi, A.; Capria, E.; Mak, L. H.; Dodhia, V. R.; Sadeghi, S. J.; Collins, S.; Somers, G.; Huq, E.; Gilardi, G. *Anal. Chem.* **2010**, *82*, 10222-10227.
(38) Niwa, T.; Shiraga, T.; Yamasaki, S.; Ishibashi, K.; Ohno, Y.; Kagayama, A. *Xenobiotica* **2003**, *33*, 717-729.
(39) Krauser, J. A.; Guengerich, F. P. *J. Biol. Chem.* **2005**, *280*, 19496-19506.
(40) Krauser, J. A.; Voehler, M.; Tseng, L.-H.; Schefer, A. B.; Godejohann, M.; Guengerich, F. P. *Eur. J. Biochem.* **2004**, *271*, 3962-3969.
(41) Sata, F.; Sapone, A.; Elizondo, G.; Stocker, P.; Miller, V. P.; Zheng, W.; Raunio, H.; Crespi, C. L.; Gonzalez, F. J. *Clin. Pharmacol. Ther.* **2000**, *67*, 48-56.

For TOC only

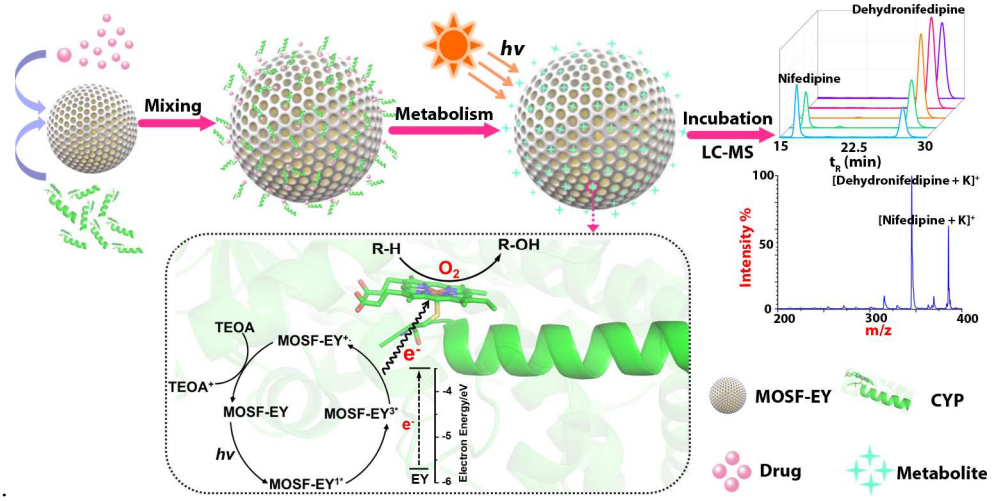
Mixing
Metabolism
hv
Incubation
LC-MS
Dehydronifedipine
Nifedipine
15
22.5
30
t_R (min)
[Dehydronifedipine + K]⁺
[Nifedipine + K]⁺
Intensity %
100
50
0
200
300
400
m/z
R-H
R-OH
O_2
TEOA
MOSF-EY*
TEOA⁺
MOSF-EY
MOSF-EY³*
MOSF-EY¹*
hv
e⁻
EY
-4
-5
-6
Electron Energy/eV
MOSF-EY
CYP
Drug
Metabolite